17th World Conference on Earthquake Engineering, 17WCEE
Sendai, Japan - September 13th to 18th 2020

SIMPLE MODELING OF PHASE AND AMPLITUDE SPECTRA FOR OBSERVED TSUNAMI WAVES

H. Sugino(1) , Y. Abe(2)

(1) *Senior Researcher, Regulatory Standard and Research Department, Secretariat of Nuclear Regulation Authority (S/NRA/R), hideharu_sugino@nsr.go.jp*
(2) *Itochu Techno-Solutions Corporation, yuta.abe.150@ctc-g.co.jp*

Abstract

An artificial tsunami wave that takes into account an amplitude associated with a certain level of tsunami hazard and the variety in waveform is important for tsunami fragility assessment which constitutes a key part of probabilistic tsunami risk assessment for nuclear power plants. To investigate the methodology of developing an artificial tsunami wave, the phase spectrum modeling method proposed by Sato et al. (2000) is applied to generate artificial tsunami waves corresponding to those observed during the 2011 Tohoku tsunami; this method generates artificial ground motions compatible with a target response spectrum.

Sato et al. (2000) used the phase spectrum modeling method to generate artificial ground motion. They considered that the average and standard deviations of the group delay time express the centroid and the duration of the wave in the time domain, respectively. Then, they separated the observed ground motions into component waves for each frequency domain, called "scale factor," using the wavelet-transform method; developed the probability model of the group delay time; and simulated this model using random sampling via the Monte Carlo method.

Herein, we first obtained a model of group delay time by applying Sato et al.'s (2000) method to the observed tsunami waves and simulated the reconstructed wave from the amplitude spectrum of the observed waves. Further, to check the influence of the group delay time model's standard deviations on the waves in the time domain, we determined the reconstructed wave for zero deviations and found almost no difference between two types of the reconstructed waves. Thus, the standard deviation of the group delay time model has extremely small influence. In addition, good reproducibility was not confirmed from the comparison of the reconstructed waves with the observed ones.

Therefore, we confirmed the changes in the reproducibility of reconstructed waves when the resolution of the group delay time model was gradually increased by dividing each scale factor domain into two and four divisions, with one average value used for each division in scale factor. We also confirmed that the degree of reproducibility tended to improve as the resolution was enhanced. Qualitatively, the reconstructed wave for 16 divisions almost matched the observed tsunami wave. We found that in phase spectrum modeling, reproducing the original tsunami wave by increasing the average value resolution was better than using the standard deviation of the group delay time. We attributed the different tendencies between the ground motion and tsunami wave to the different frequency bands in each wave. We also observed nearly identical tendencies in amplitude spectrum modeling.

We obtained basic knowledge regarding phase and amplitude spectra modeling for observed tsunami waves. Based on these results, we will develop a methodology to generate an artificial tsunami wave corresponding to a certain level of tsunami hazard.

Keywords: Tsunami, Phase spectrum, Amplitude spectrum, Group delay time, Wavelet transform

1. Introduction

The tsunami triggered by the 2011 off the Pacific coast of Tohoku Earthquake that occurred on March 11, 2011 (hereafter "Tohoku earthquake tsunami"), caused a serious accident at the Fukushima Daiichi Nuclear Power Plant of Tokyo Electric Power Company. The government report on this accident [1] drew the following lessons from it: the existence of a risk where a tsunami that exceeds the expectation of the facility design should be fully recognized and measures to ensure the maintenance of important safety functions, even if its premises are flooded and hit by destructive runup waves, should be taken, and risk management that utilizes probabilistic risk assessment (PRA) should be conducted.

Methods for a quantitative evaluation of the tsunami risk at nuclear power plants include the standard for Procedure of Tsunami Probabilistic Safety Assessment for nuclear power plants by the Atomic Energy Society of Japan [2]. The tsunami PRA evaluates the frequencies of the reactor core damage or the loss of reactor containment vessel function and quantifies the comprehensive tsunami risk of a nuclear power plant by combining the following three analysis methods: the probabilistic tsunami hazard (hereafter "tsunami hazard") analysis method, which evaluates the relation between the strength of the tsunami (such as its height) that attacks the facility under analysis and the frequency of the occurrence of tsunamis that exceed its strength; the tsunami fragility analysis method, which evaluates the probability of function loss of structures and components; and the accident sequence analysis method, which evaluates the probability of damage to the reactor core, accounting for the safety function of the plant system.

The abovementioned three analysis methods are interrelated. Especially, the tsunami fragility analysis method requires varied information related to the function loss, such as the depth of flooding at each installation location of structures and components, flow velocity, and wave pressure, in relation to the given tsunami's strength level. To obtain the information through tsunami runup analysis, chronological waveform of the sea-surface water level that simulates the tsunami (hereafter "artificial tsunami wave") is necessary as its input condition. Moreover, these artificial tsunami waves must be related to the tsunami hazard information.

The method of multiplying the standing waveform, obtained using the amplitude spectrum defined through the observed seismic motion and the phase spectrum given by a uniform random number, with the amplitude envelope, which represents the phase characteristics of seismic motion, has been used for producing the artificial seismic motion in the field of seismic design of buildings/structures of nuclear power plant facilities [3]. Moreover, various methods that focus on the phase characteristics of the observed seismic motion, to achieve more realistic phase characteristics, have been proposed. For instance, Sato et al. [4] indicated that the average and standard deviations of group delay time, which is defined as the inclination of the Fourier phase spectrum in the angular frequency domain, express the centroid and expansion (duration) of seismic motion in the time domain, and proposed a modeling method of the phase spectrum based on the observed seismic wave that utilizes wavelet transformation [5]. This method is used in the seismic design of railway structures [6]. As seen in this example, a PRA method related to seismic motion [7] can produce artificial seismic motion related to the earthquake hazard level of each exceedance probability by applying these production methods of artificial seismic motion and utilizing the uniform hazard spectrum evaluated through the probabilistic earthquake hazard analysis. Furthermore, by conducting an earthquake response analysis of buildings/structures that uses these as its inputs, a continuous evaluation method from the probabilistic earthquake hazard analysis to the fragility analysis has been established.

Meanwhile, in the field of tsunami, Sugino et al. [8] proposed a tsunami fragility analysis method based on the tsunami runup analysis as part of preparation of the tsunami PRA. This method evaluates varied information, such as flooding depth, at the installation positions of structures (hereafter "response value") through tsunami runup analysis, and analytically calculates the tsunami fragility curve based on the averages and standard deviations of the response values of several input waveforms and those of the proof stress value related to the function loss of structures. In this method, many sine waves that modulated amplitude and wavelength are used due to the necessity to consider the uncertainties in input waveforms as the input condition of tsunami runup analysis. While sine wave is an artificial tsunami waveform that extremely simplifies the non-stationary tsunami waveform, it is difficult to say that it accounts for the geographical characteristics around the site to be analyzed, which are related to the occurrence of tsunami.

To improve the explainability of the tsunami PRA, an artificial tsunami waveform that accounts for the geographical characteristics around the site to be analyzed is necessary even for the tsunami runup analysis used for tsunami fragility analysis instead of the abovementioned sine wave. However, hardly any study has focused on the production method of artificial tsunami waveforms, or even on the modeling of the phase/amplitude spectrum of the tsunami waveform, that can be used as their basic data.

This study examined the production methods of the phase spectrum model of the observed tsunami waveform of the Tohoku earthquake tsunami while referring to Sato et al.'s method [4], to obtain basic data toward the construction of a production method of artificial tsunami waveforms. Moreover, it examined the production method of the amplitude spectrum model of tsunami waveforms. Furthermore, it compared the reconstructed waveform, which applied these methods, and the observed tsunami waveform and verified its validity through the extent of its reproducibility.

2. Procedure from the production of phase/amplitude spectrum models to reconstruction of waveform

Fig.1 shows the procedure from the production of phase/amplitude spectrum models using the observed tsunami waveform to the reconstruction of the waveform using these models. This procedure comprises the following four parts: (1) preprocessing of the observed tsunami waveform, (2) production of phase spectrum model, (3) production of amplitude spectrum model, and (4) reconstruction of waveform. Each part is discussed in detail below.

(1) Preprocessing method of the observed tsunami waveform

As discussed earlier, the artificial tsunami waveform is an input condition of the tsunami runup analysis for tsunami fragility analysis, and is defined at the evaluation location of the tsunami hazard. Thus, it is necessary to set the duration of the artificial tsunami waveform and the appearance time of its maximum water level while accounting for the propagation time of the tsunami required for the artificial tsunami waveform to reach the shore from the input location and then back. Here, the water-level waveform observed by a GPS buoy during the Tohoku earthquake tsunami [9] was used to obtain the necessary information of waveform (mainly the phase/amplitude information, and duration) from the observed tsunami waveform. The first half of these observed tsunami waveforms include the waves that directly arrived at the observation point from the source area of the tsunami, and their second half includes the waves that passed the observation point, arrived at the shore, reflected there, and reached the observation point again. Thus, to extract only the first half, the following processes will be conducted.

1) Shift the time of the observed tsunami waveform such that the appearance time of its maximum water level becomes 1500 s.
2) Extract the observed tsunami waveforms from t = 0 to 3000 s after the shift and set the duration T at 3000 s.
3) Conduct a tapering with the sine wave from the starting point to 600 s, to make the amplitude of the extracted observed tsunami waveform at the starting point t = 0 s gradually increase from zero. Similarly, taper with the cosine wave from the last 600 s until the end point, so that the amplitude at the end point t = 3000 s gradually decrease to zero.
4) Add zero data after 3000 s, and then, set the total data number at 2^{15} and the total data time T_d at 163840 (=5 x 2^{15}) s.

(2) Production method of phase spectrum model

Sato et al. [4] used wavelet transformation and inverse transformation [5] to extract phase information from non-stationary waveforms, such as the observed seismic motion. By using the scaling and shifting of function $\varphi(t)$, called the mother wavelet, wavelet transformation can extract waveforms that are analogous to the mother wavelet at various scales within the time history data x (t) without losing the time information. As the observed tsunami waveform is similar to a non-stationary waveform, and we refer to this method while improving its parts. Here, a general outline of Sato et al.'s [4] method is discussed first,

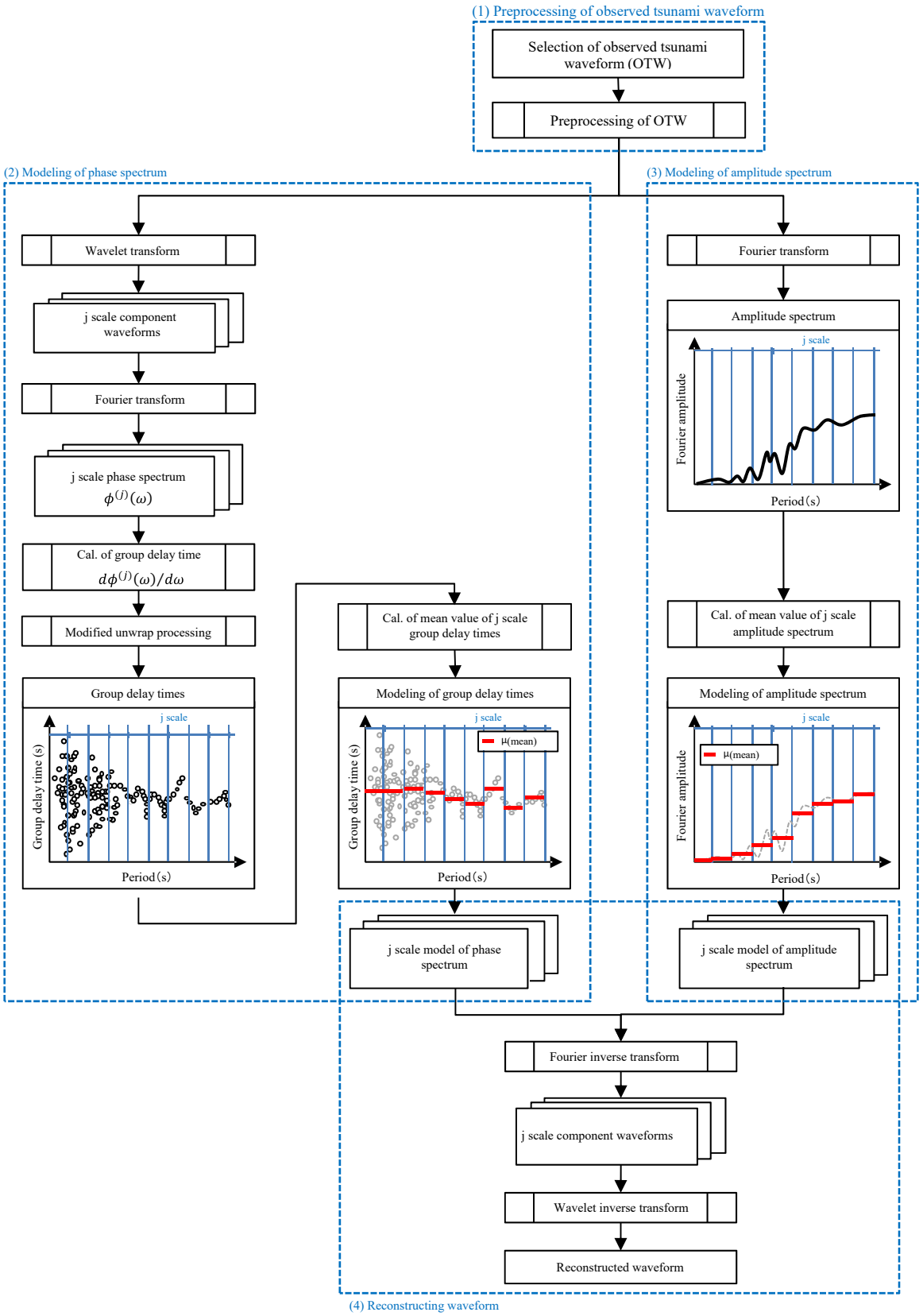

Fig. 1 – Production procedure of reconstructed waveform using the phase and amplitude spectrum models

followed by the explanation of the points where changes were made.

First, time history data $x(t)$ must go through wavelet transformation and resolved into component waveforms at each scale factor j. The dispersion wavelet transformation and inverse transformation of $x(t)$ can be expressed as

$$w_k^{(j)} = \int_{-\infty}^{\infty} x(t)\, \varphi_{j,k}^*(t) dt \tag{1}$$

$$x(t) = \sum_j g^{(j)}(t) = \sum_j \sum_k w_k^{(j)}\, \varphi_{j,k}(t) \tag{2}$$

Here, $\varphi(t)$ represents the mother wavelet, * represents the complex conjugate, suffix j represents the scale factor, suffix k represents the time position, and $w_k^{(j)}$ represents the wavelet coefficient at j dimension. j indicates the roughness (resolution) of the signal and $\varphi_{j,k}$(t) is a wavelet of a different resolution. The time history data $g^{(j)}(t)$ at the scale factor j can be expressed in Eq. (3), and is called the wavelet component. Note that in this paper, WAVELAB850 of Buckheit et al. [10] is used as a tool for wavelet transformation and inverse transformation:

$$g^{(j)}(t) = \sum_k w_k^{(j)} \varphi_{j,k}(t) \tag{3}$$

Next, each component waveform is Fourier transformed to obtain the phase spectrum $\phi^{(j)}(\omega)$ of the scale factor j. Then, $\phi^{(j)}(\omega)$ is differentiated with the angular frequency ω to obtain the group delay time ${t_{gr}}^{(j)}(\omega)$, and the unwrapping method of Sawada et al. [11] is applied to calculate the average $\mu^{(j)}$ and standard deviation $\sigma^{(j)}$ of group delay time at the support section $f^{(j)}$ of the scale factor j.

Meyer [12] is applied as the mother wavelet $\varphi(t)$. In such a case, $\varphi(t)$ becomes the compact support in the frequency domain. In this support section, $f^{(j)}$(1/s) can be expressed as

$$\left\{ \frac{2^j}{3T_d} \le f^{(j)} \le \frac{2^{j+2}}{3T_d} \right\} \tag{4}$$

Here, T_d represents the total time of the time history data.

At the support section $f^{(j)}$ of Eq. (4), there are two values: the phase spectrum and group delay time overlap at the neighboring scale factor j. Thus, the support section $f^{(j)}$ of Eq. (5) is defined such that the phase spectrum and amplitude spectrum have 1:1 correspondence.

$$\left\{ \frac{2^{j-1}}{T_d} \le f^{(j)} \le \frac{2^j}{T_d} \right\} \tag{5}$$

The average $\mu^{(j)}$ and standard deviation $\sigma^{(j)}$ of the group delay time are calculated using the data in the support section $f^{(j)}$ of Eq. (5).

Next, the same procedure is applied to several observed seismic motions, a regression model equation is obtained based on the data group of average $\mu^{(j)}$ and standard deviation $\sigma^{(j)}$, and the group delay time model ${t'}_{gr}{}^{(j)}(\omega)$ is obtained using the Monte Carlo method. By integrating this group delay time model ${t'}_{gr}{}^{(j)}(\omega)$ with ω, the phase spectrum model $\phi'^{(j)}(\omega)$ of the scale factor j is obtained. That's Sato et al.'s [4] method.

As this study partially improves Sato et al.'s method, these changes must be explained. First, the improvement in the unwrapping method is discussed. Sawada et al. [11] initially obtained ${t_{gr}}^{(j)}(\omega)$, produced its histogram, and conducted $\pm T$ time shift to the data outside the region of $[({T_{mod}}^{(j)} - T/2)\sim({T_{mod}}^{(j)} + T/2)]$ centered around the mode ${T_{mod}}^{(j)}$ in order for the data to fit within this region. This time shift is equivalent to $\pm 2\,\pi T/T_d$ (rad) shift, and any shift other than $\pm 2\pi$ would overwrite the phase information originally contained by the tsunami waveform. Therefore, the following improvement was made to prevent the unwrapping method from changing the phase information of the originally observed tsunami waveform. The mode ${T_{mod}}^{(j)}$ of the histogram of the group delay time ${t_{gr}}^{(j)}$ is changed to the median ${T_{mid}}^{(j)}$. Moreover, for the data to fit within the region of $[({T_{mid}}^{(j)} - T_d/2)\sim({T_{mid}}^{(j)} + T_d/2)]$ centered around the median ${T_{mid}}^{(j)}$, the shift conducted on the data outside this region in order to make them fit within it is changed to $\pm T_d$. The reason for changing from ${T_{mod}}^{(j)}$ to ${T_{mid}}^{(j)}$ is that when the scale factor j is within the region from 2 to 4, there is little data, and therefore, the histogram can be biased. In this case, the average would also be set at the edge of the distribution. Such cases should be avoided as much as possible. Moreover, $\pm T_d$ is equivalent to $\pm 2\pi$ (rad) shift; therefore, the phase information of the observed tsunami waveform is retained as it is.

Next, the production of the group delay time model ${t'_{gr}}^{(j)}(\omega)$ by Sato et al. [4] uses the regression model equation obtained based on the data group of average $\mu^{(j)}$ and standard deviation $\sigma^{(j)}$ calculated from several observed seismic motions. While the part where a regression model equation is obtained will be left as a future challenge, this study nevertheless proposes a model where only the average $\mu^{(j)}$ of group delay time is used and its standard deviation $\sigma^{(j)}$ is omitted, which is a simpler version of the group delay time model. However, note that the support section $f^{(j)}$ of the scale factor j is divided into several parts, and a method that produces an expression with as small as possible division while taking the relationship between the division number and the reproducibility of the reconstructed waveform into account is proposed.

(3) Production method of amplitude spectrum model

No existing research on the amplitude spectrum model of the tsunami waveform is known. Therefore, an amplitude spectrum model that matches the aforementioned phase spectrum production method is proposed. First, the observed tsunami waveform is Fourier transformed to obtain the amplitude spectrum $A(\omega)$. Next, similarly to the group delay time model ${t'_{gr}}^{(j)}(\omega)$ discussed above, a support section $f^{(j)}$ is set and then divided into several parts. The average $\mu^{(j)}$ of each part is calculated using the amplitude spectrum, which is set as the amplitude spectrum model $A'^{(j)}(\omega)$. While the method described here is relatively simple, the fact that a reconstructed waveform that used such an amplitude spectrum model can reproduce the original observed tsunami waveform to a certain extent will be discussed later in this paper.

(4) Waveform reconstruction method using the phase/amplitude spectrum models

The waveform reconstruction is conducted using the phase spectrum model $\phi'^{(j)}(\omega)$ and the amplitude spectrum model $A'^{(j)}(\omega)$ obtained through the methods of Eq. (2) and Eq. (3) discussed above. First, the phase spectrum model $\phi'^{(j)}(\omega)$ and the amplitude spectrum model $A'^{(j)}(\omega)$ with the same scale factor j are used to conduct Fourier inverse transformation in order to obtain the component waveform $g'^{(j)}(t)$ after the modeling. Next, obtain the reconstructed wave $x'(t)$ through Eq. (6), which replaced $g^{(j)}(t)$ in wavelet inverse transformation Eq. (2) with $g'^{(j)}(t)$.

$$x'(t) = \sum_j g'^{(j)}(t) \tag{6}$$

3. Test calculation example of reconstructed waveform using the phase/amplitude spectrum models

3.1 Observed tsunami waveform and its preprocessing

In this paper, G804 (off the coast of central Iwate), among the tsunami waveforms observed by the GPS buoy during the Tohoku earthquake tsunami [9], is studied. Fig.2 shows the position where the GPS buoy was installed. In addition, Fig.3 shows the observed tsunami waveform after the aforementioned process. This figure shows that the appearance time of the maximum water level was shifted to 1500 s and that the starting/end points of the waveform were at zero after a gradual increase/decrease achieved by tapering. Moreover, zero data were added when the duration T was 3000 s and after that. The total data number was 2^{15}, and the total time of the time history data T_d was 163840 (=5 x 2^{15}) s.

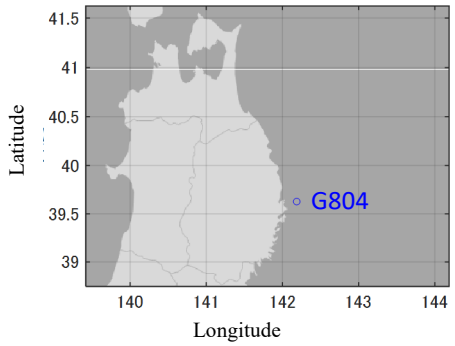

Fig. 2 – Installation position of G804 (off the coast of central Iwate)

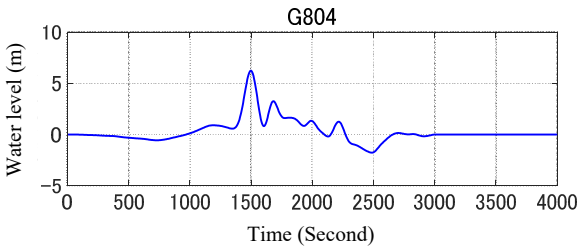

Fig. 3 – Observed tsunami waveform at G804

3.2 Examination of phase spectrum model

In this section, the production method of the phase spectrum model shown in Fig.1 is examined. For this purpose, the amplitude spectrum model of this figure is replaced by that of the observed tsunami waveform, reconstructed waveforms are created using various phase spectrum models and compared to the original observed waveform, in order to focus only on the phase spectrum model production methods and verify their influence/effect.

First, similar to the method of Sato et al. [4], the normal distribution was postulated using the average $\mu^{(j)}$ and standard deviation $\sigma^{(j)}$ of the group delay time of each support section $f^{(j)}$, and the group delay time model and reconstructed wave were calculated through random sampling. For the generation of a normal random number, the function randn [15] of MATLAB by the Mersenne Twister method [14] was used. Fig.4 (a) shows the group delay time model, and Fig.4 (b) shows the reconstructed waveform. Next, to verify the effect of the standard deviation $\sigma^{(j)}$ on the group delay time model, a group delay time model and reconstructed waveform based on the average $\mu^{(j)}$ of the group delay time alone were also obtained. These calculation results are shown in Fig.5 (a) and Fig.5 (b). In Fig.4 (a) and Fig.5 (a), the red solid line represents $\mu^{(j)}$, the green broken line represents $\pm 1\sigma^{(j)}$, and the blue circle represents the group delay time model. In the same figures, the degree of the scale factor j and its support section $f^{(j)}$ are also shown. In Fig.4 (b) and Fig.5 (b), the red solid line represents the reconstructed waveform and blue solid line represents the observed tsunami waveform.

When the reconstructed waveforms of Fig.4 (b) and Fig.5 (b) are compared, it is verified that they are similar to the point of being indistinguishable. This fact indicates that including the standard deviation $\sigma^{(j)}$ in model production has little effect. Moreover, when these reconstructed waveforms are compared to the original observed waveform, while the waveforms are similar during 200 s at the appearance time of the maximum water level, which is around 1500 s, they do not match at other times. Thus, the reproducibility for the observed tsunami waveform is low.

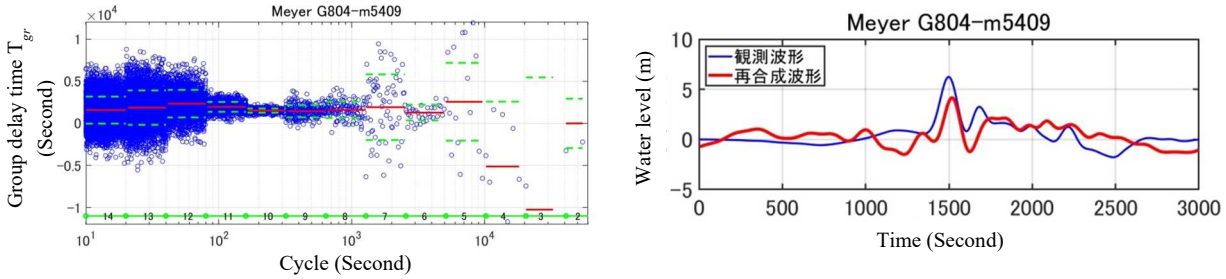

(a) Group delay time model (b) Reconstructed waveform and observed waveform

Fig. 4 – Group delay time model obtained by random sampling and reconstructed waveform

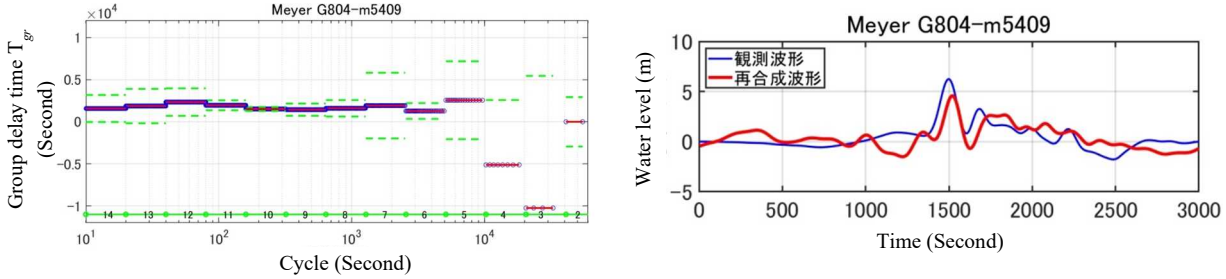

(a) Group delay time model (b) Reconstructed waveform and observed waveform

Fig. 5 – Group delay time model based only on the average and reconstructed waveform

Next, Fig.6 and Fig.7 show the cases where the resolution of the average is increased by dividing the support section $f^{(j)}$ of each scale factor j into two and four, which is the method proposed in this paper. Fig. 6 (a) and Fig.7 (a) show the group delay time models with two and four divisions, respectively. In the figures, the same red solid line and green broken line included in Fig.4(a) are shown. They represent $\mu^{(j)}$ and $\sigma^{(j)}$ of $f^{(j)}$ obtained from the group delay time of the original observed tsunami waveform. The act of dividing the support section $f^{(j)}$ indicates the approximation toward the distribution of the group delay time of the observed tsunami waveform following the increase in divisions from the side with smaller degree of the scale factor j (long cycle side). Similarly, Fig.6 (b) and Fig.7 (b) also show the reconstructed waveforms obtained through two and four divisions. The reconstructed waveform of Fig.6 (b) showed an improvement in the maximum water level around 1500 s, compared to that shown in Fig.5 (b). However, reproducibility was still low. However, the reconstructed waveform of Fig.7 (b) showed improvement in matching with the phase and amplitude of the observed tsunami waveform, and its reproducibility is considerably higher. Moreover, it was verified that further increase in the number of division improves the reproducibility.

Thus, it was clarified that when producing a phase spectrum model, increasing the resolution of the average results in better reproducibility for the original observed tsunami waveform compared to using the standard deviation of group delay time. The reason why this knowledge differs from that obtained when the standard deviation of group delay time was used by Sato et al. [4] is attributed to the difference between the periodic bands of the waveform of seismic motion and that of the tsunami. Namely, while their study mainly focused on seismic motion, which is an acceleration waveform comprising short cycle waveforms, the water-level waveform of the tsunami comprises long-cycle waveforms.

3.3 Examination of amplitude spectrum model

In this section, the production method of the amplitude spectrum model is examined. For this purpose, the reconstructed wave is produced using various amplitude spectrum models and phase spectrum of the observed tsunami waveform while accounting for the concordance with the production method of the phase

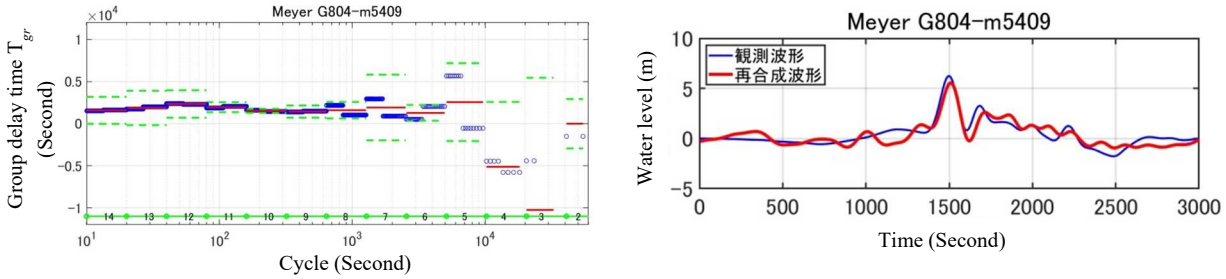

(a) Group delay time model (b) Reconstructed waveform and observed waveform

Fig. 6 – Group delay time model based on the average of two divisions and reconstructed waveform

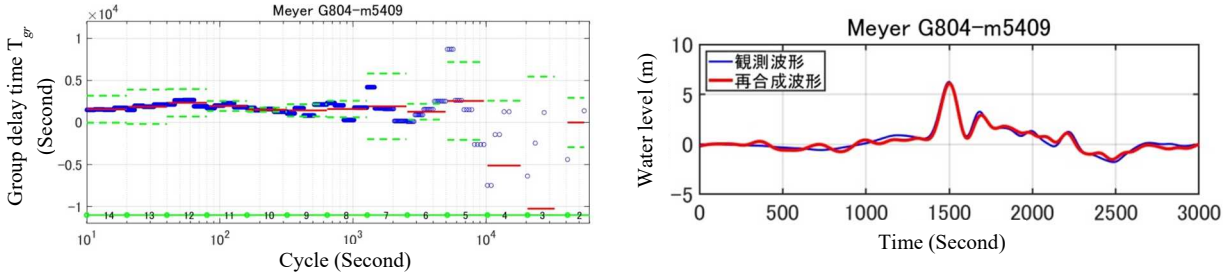

(a) Group delay time model (b) Reconstructed waveform and observed waveform

Fig. 7 – Group delay time model based on the average of four divisions and reconstructed waveform

spectrum model discussed in Section 3.2. Then, we compare this reconstructed waveform with the original observed tsunami waveform, to focus only on the amplitude spectrum model production methods and verify their influence/effect.

Fig.8 to Fig.10 show the amplitude spectrum models and the reconstructed waveforms when the number of divisions of the support section $f^{(j)}$ of each scale factor j is gradually increased similar to the phase spectrum models.

In Fig.8 (a) to Fig.10 (a), the amplitude spectrum models are indicated by red circles and those of the observed tsunami waveform are indicated by blue circles, respectively. These figures indicate the tendency of the amplitude spectrum models to become closer to that of the observed tsunami waveform from the long-cycle side of the scale factor j 2 to 6 as the number of divisions increases.

In Fig.8 (b) to Fig.10 (b), the reconstructed waveforms produced using these amplitude spectrum models are indicated by a red solid line and the observed tsunami waveforms are indicated by a blue solid line, both of which overlap each other. Even in the case with one-division average, shown in Fig.8 (b), the main waveform is reproduced has equal level of reproducibility as that in the case of four-division average, shown in Fig.9 (b). Moreover, while the improvement in reproducibility can be observed as the number of divisions is increased, the amount of improvement is small.

These results indicate the difference in the sensitivity of the modeling method using the average between the phase spectrum model and amplitude spectrum model. Moreover, the phase spectrum is relatively more dominant over the waveform than the amplitude spectrum model.

3.4 Test calculation of reconstructed wave using phase/amplitude spectrum models

In Sections 3.2 and 3.3, only one of the phase or amplitude spectrum was modeled to produce the reconstructed waveform. This section shows the production of the reconstructed waveform by setting the division number of the support section and using their average through the methods discussed thus far, to verify its reproducibility for the observed tsunami waveform.

Fig.11 shows the reconstructed wave produced using the one division average of both the group delay time model shown in Fig.5 (a) and the amplitude spectrum model shown in Fig.8 (a). The reconstructed

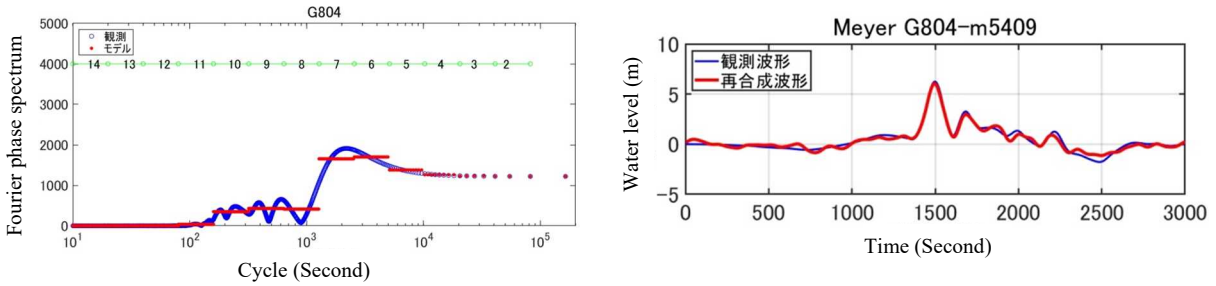

(a) Amplitude spectrum model (b) Reconstructed waveform and observed waveform

Fig. 8 – Amplitude spectrum model based on the average of one division and reconstructed waveform

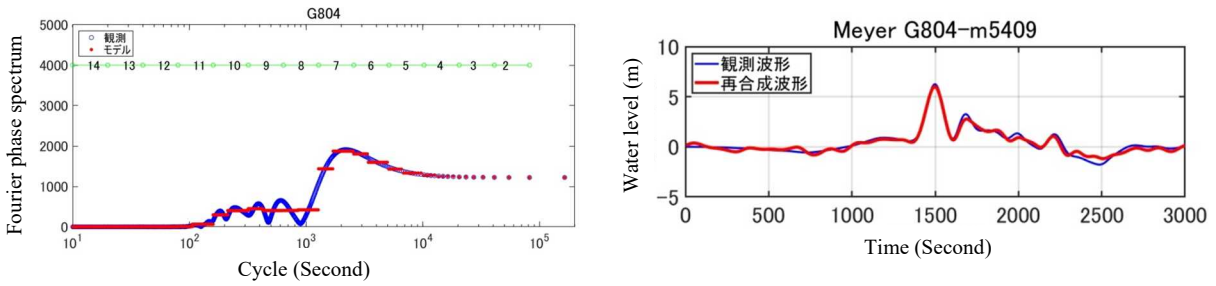

(a) Amplitude spectrum model (b) Reconstructed waveform and observed waveform

Fig. 9 – Amplitude spectrum model based on the average of two divisions and reconstructed waveform

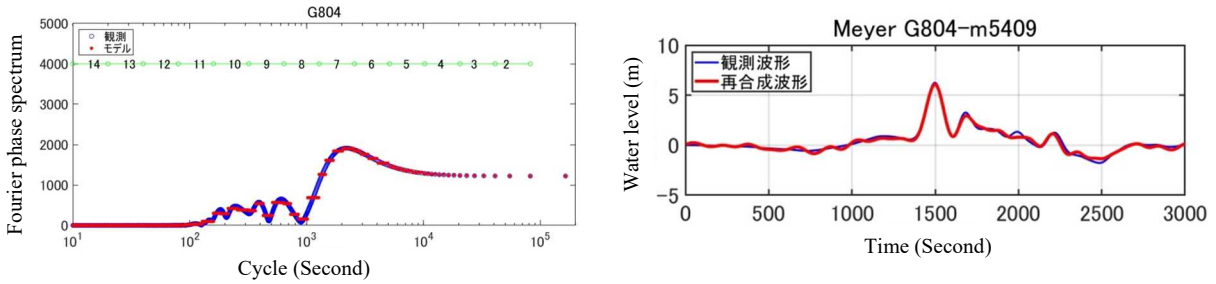

(a) Amplitude spectrum model (b) Reconstructed waveform and observed waveform

Fig. 10 – Amplitude spectrum model based on the average of four divisions and reconstructed waveform

waveform in this case closely resembles that shown in Fig.5 (b). This result also shows that the phase spectrum model is more dominant over the waveform than the amplitude spectrum model. Similarly, Fig.12 and Fig.13 show the cases with the two- and four-division averages, respectively. As the influence of the phase spectrum model is more dominant in the degree of reproducibility, they closely resemble the reconstructed waves shown in Fig.6 (b) and Fig.7 (b), and one can see how the reproducibility improves as the number of divisions increases. Moreover, it is verified that in the case of the four-division average model, the reconstructed waveform and the observed tsunami waveform mostly match.

4. Conclusion

This study examined production methods for the phase spectrum model of the observed waveform of the Tohoku earthquake tsunami while referring to Sato et al.'s [4] method, to obtain basic data for the construction of a production method of artificial tsunami waveforms. It also examined a production method for the amplitude spectrum model of tsunami waveforms. Furthermore, it compared the reconstructed waveform, which applied these methods, and the observed tsunami waveform and verified the validity of

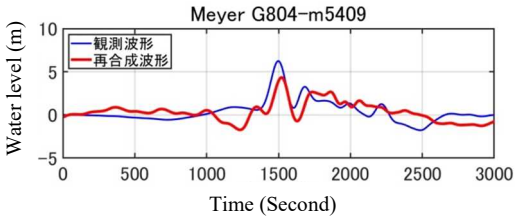

Fig. 11 – Reconstructed wave by group delay time model and amplitude spectrum model based on the average of one division

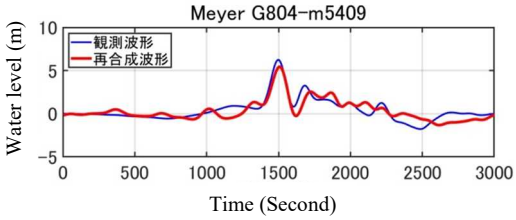

Fig. 12 – Reconstructed wave by group delay time model and amplitude spectrum model based on the average of two divisions

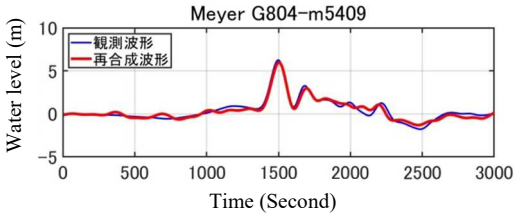

Fig. 13 – Reconstructed wave by group delay time model and amplitude spectrum model based on the average of four divisions

each model through the extent of its reproducibility.

First, the reconstructed waveform was evaluated from the group delay time model by using Sato et al.'s [4] method and the amplitude spectrum of the observed tsunami waveform. Next, the reconstructed waveform was calculated with the standard deviation at zero, only using average, to verify the influence of standard deviation on the group delay time model. The result showed that there was hardly any difference between them, indicating that the effect of standard deviation on the group delay time model was extremely small. Moreover, when these reconstructed waveforms and the original observed tsunami waveform were compared, good reproducibility could not be verified. Next, when the resolution was improved by replacing one average for each scale factor, with an average of two or four divisions of the support section, the reproducibility tended to improve. Qualitatively, it was verified that the result of the four divisions mostly matched that of the observed tsunami waveform. Thus, it was elucidated that the usage improvement of the resolution of the average resulted in better reproducibility for the original observed tsunami waveform as compared to the usage of the standard deviation of the group delay time model. It was inferred that seismic motion and tsunami tend to differ due to the difference in the frequency band of each waveform.

Furthermore, it was observed that the reproducibility level similarly improved in the production method of the amplitude spectrum model when the number of divisions was increased. However, as its reproducibility was already good at the point of one division, the extent of improvement was small. From these results, the difference in the method's sensitivity using the average between the phase spectrum model and amplitude spectrum model was observed. Moreover, the phase spectrum was found to be relatively more dominant over the waveform than the amplitude spectrum model.

These results provided the basic knowledge that simple modeling using the average of group delay time and the average of amplitude spectrum is effective as a production method for the phase/amplitude spectrum model of the observed tsunami waveform. While this study only focused on one tsunami waveform, in the

future, this knowledge will form the basis for calculating average and standard deviation of the group delay time and amplitude spectrum of several tsunami waveforms, to construct a production method for the artificial tsunami waveform that integrates these as an uncertainty.

Acknowledgements

For the preparation of this paper, we used the observed waveform data of the tsunami of the earthquake off the Pacific coast of Tohoku published in the Nationwide Ocean Wave Information Network For Ports And Harbours (NOWPHAS) of the Ports and Harbours Bureau of the Ministry of Land, Infrastructure, Transport and Tourism (MLIT). Moreover, for the wavelet transformation and inverse transformation used in the analysis of the tsunami waveform data, WAVELAB850 published by Stanford University was used. We express our gratitude to Dr. Yoshitaka Murono of the Railway Technical Research Institute, who instructed us on the unwrapping method of group delay time. Please note that this paper brought together achievements of the 2015 study on the inspection standard for earthquake/tsunami resistant design of nuclear power plant facilities (Analysis of observed tsunami waveform and production of artificial tsunami waveform) by the Secretariat of the Nuclear Regulation Authority.

References

[1] Nuclear Emergency Response Headquarters, Goverment of Japan (2011): Report of Japanese Government to the IAEA Ministerial Conference on Nuclear Safety – The accident at TEPCO's Fukushima Nuclear Power Stations -.

[2] Atomic Energy Society of Japan (2017): *A standard for Procedure of Tsunami Probabilistic Safety Assessment for nuclear power plants 2016* (in Japanese).

[3] Oosaki Y (1984): Guideline for Assessment of Design Basis Ground Motion for Nuclear Power Plants. Especially Regarding Oosaki Spectrum, *Research Report of ORI*, 84-01.

[4] Sato T, Murono Y, Nisimura A (2000): Empirical Modeling of Phase Spectrum of Earthquake Motion. *Journal of Japan Society of Civil Engineers,* **640** (I-50), 119-130 (in Japanese).

[5] Sasaki F, Maeda T, Yamada M (1992): Study of Time History Data Using Wavelet Transform. *Journal of Structural and Construction Engineering*, **38B**, 9-20 (in Japanese).

[6] Railway Technical Research Institute (2012): *Design Standards for Railway Structures and Commentary (Seismic Design)*, Maruzen Publishing.

[7] Atomic Energy Society of Japan (2015): A standard for Procedure of Seismic Probabilistic Safety Assessment for nuclear power plants 2015 (in Japanese).

[8] Sugino H, Iwabuchi Y, Nishio M, Tsutsumi H, Sakagami M, Ebisawa K (2008): Development of probabilistic methodology for evaluating tsunami risk on nuclear power plants. *The 14th World Conference on Earthquake Engineering (14WCEE)*, Beijing, China.

[9] Kawai H, Satoh M, Kawaguchi K, Seki K (2011): The 2011 off the Pacific Coast of Tohoku Earthquake Tsunami Observed by GPS Buoys. *Journal of Japan Society of Civil Engineers (B2: Costal Engineers)*, **67** (2), I_1291-I_1295.

[10] Buckheit J, Chen S, Donoho D, Johnstone I (2005): *About WaveLab (version 850)*, Stanford University & Jeffrey Scargle NASA-Ames Research Center.

[11] Sawada S, Morikawa H, Toki K, Yokoyama K (1998): Identification of Path and Local Site Efects on Phase Spectrum of Seismic Motion. *The 10th Earthquake Engineering Symposium Proceedings*, 915-921.

[12] Meyer Y (1989): *Orthonormal Wavelets*. Springer, 21-27.

[13] Matsumoto M, Nishimura T (1998): Mersenne Twister: A 623-Dimensionally Equidistributed Uniform Pseudorandom Number Generator. *ACM Transactions on Modeling and Computer Simulation*, **8** (1), 3-30.

[14] The MathWorks, *MATLAB Documentation "Function"*.

